Organic Electronics 32 (2016) 258–266

Contents lists available at ScienceDirect

Organic Electronics

journal homepage: www.elsevier.com/locate/orgel

Organic soluble indigoids derived from 3-hydroxybenzaldehyde for N-type organic field-effect transistor (OFET) applications

Jenner H.L. Ngai [a], Louis M. Leung [a, *], S.K. So [b], Harrison K.H. Lee [b]

[a] Department of Chemistry, Hong Kong Baptist University, Kowloon, Hong Kong SAR, China
[b] Department of Physics, Hong Kong Baptist University, Kowloon, Hong Kong SAR, China

ARTICLE INFO

Article history:
Received 2 December 2015
Received in revised form
23 February 2016
Accepted 23 February 2016
Available online xxx

Keywords:
OFET
Baeyer Drewson indigo synthesis
3-Hydroxybenzaldehyde
Organic semiconductors
Organic soluble indigoids

ABSTRACT

Two new series of organic soluble indigoids 7-7′-dialkoxyindigoids (**2a, 2b**) and 4,4′-dibromo-7,7′-dialkoxyindigoids (**3a, 3b**) (alkoxy = *n*-butoxy and *n*-octyloxy) were synthesized starting from the inexpensive 3-hydroxybenzaldehyde. The indigoids were soluble in common organic solvents including chloroform, dichloromethane, toluene, ethyl acetate and ethers. The enhanced solubility was suggested to be a lack of intermolecular hydrogen-bonds as confirmed by single crystal X-ray diffraction analyses. It was found that intramolecular hydrogen-bonds in indigoids are crucial to the exhibition of field-effect in OFETs, while intermolecular hydrogen-bonds only caused insolubility of the indigoids. Compared to the pristine insoluble indigo (LUMO = −3.55 eV and E_g = 1.91 eV), the soluble indigoids containing electron donating alkoxy side chains at the indigoid 7 and 7′ positions were shown to have their LUMO decreased by −0.13 to −0.26 eV. Among the indigoid studied, the soluble indigoid **3a** containing electron donating alkoxy side chains at the indigoid 7 and 7′ positions and bromine groups at the indigoid 4 and 4′ positions exihibited a narrowest bandgap energy with E_g = 1.66 eV. Employing the same fabrication technique and a bottom-gate-top-contact OFET configuration, the soluble indigoids were found to have electron mobility similar to and within an order of magnitude of the pristine indigo.

1. Introduction

Indigo is a natural occurring blue pigment that has found applications since ancient times including in the wrappings for Egyptian mummies [1].In order to prepare the dye , the leaves and stalks of the harvested plants were submerged in water for fermentation. The bio-matters eventually produced glucose containing indoxyl. Followed by hydrolysis and oxidation, the indoxyl compounds finally converted to indigo. Indigo is a durable, air stable, non-toxic and biodegradable blue dye.

Recently, it was recognized that indigo was an effective ambipolar and biodegradable semiconductor with hole and electron mobility reported to be 0.02 $cm^2 V^{-1} s^{-1}$. It has been successfully applied as an active layer for n-type organic field-effect transistors (OFET) [2,3]. The field-effect observed in its OFET is a result of high electron or hole mobility modulated by an external electric field. Indigo is an electron deficient compound that has low-lying LUMO thus making it an excellent electron acceptor for n-type organic electronic devices. The compound itself, however, is not soluble in organic solvents and thus has limited processability. The poor solubility was attributed to the extensive intermolecular hydrogen-bonds between the indigo molecules. Several attempts to improve its solubility [4–6], however, were failed in creating an organic soluble indigo derivative while preserving the conductive indigoid (or indigotin) chromophore. Reactions on indigo usually took place at the most reactive analogous amide 1 and 1′ positions (see Fig. 1), and thus destroying the inter- and intramolecular hydrogen-bonds within the indigo molecules [7–9]. Direct halogenation of indigo has also been reported under harsh conditions [10,11], but the products remained insoluble in organic solvents. Thus mading it impossible to further functionalize the indigo moiety. Sulfonation was by far the most facile reaction in producing a water soluble indigo derivative [12]. The sulfonated indigo known as “indigo carmine” has been applied as electrode materials for rechargeable batteries. Indigo carmine, however, is not soluble in organic solvents and the moisture sensitive hydrophilic protic sulfonic acid groups are detrimental for charge transport in n-type organic semiconductor applications.

* Corresponding author.
E-mail addresses: jennerngai@gmail.com (J.H.L. Ngai), s20974@hkbu.edu.hk (L.M. Leung).

http://dx.doi.org/10.1016/j.orgel.2016.02.035
1566-1199/

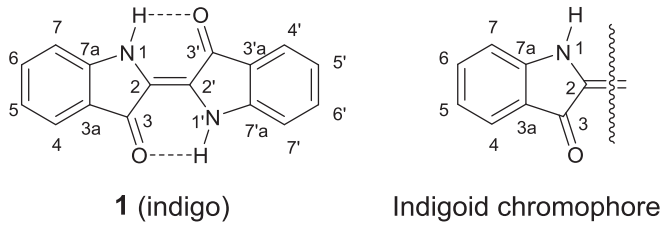

Fig. 1. Compound **1** (indigo) with intramolecular hydrogen-bonds and the indigoid chromophore under IUPAC fused ring numbering system.

Moreover, p-type organic semiconductors such as polythiophenes, tetracene, pentacene, rubrene and CuPc are readily available while there are only few n-type organic semiconductors including PCBM, ICBA, ICMA have been reported. In this report, the synthesis of two series of organic soluble indigoids (see Fig. 2) including 7,7′-dialkoxyindigoids (**2a, 2b**) and 4,4′-dibromo-7,7′-dialkoxyindigoids (**3a, 3b**) is being reported. The electron mobility of the novel electron accepting n-type materials was measured by the fabrication of n-type OFET.

2. Results and discussion

2.1. Synthesis

An inexpensive 3-hydroxybenzaldehyde (**3-HBA**) was used as the starting material for the synthesis of 7,7′-dialkoxyindigoids (**2a-b**). An Ullmann type etherification [13] was performed on **3-HBA** using DMF as the solvent to give the corresponding *n*-butoxy and *n*-octyloxy benzaldehyde (**5a-b**) with 90–95% yield. Nitration on **5a-b** was carried out with a nitrating reagent [14] to give the alkoxynitrobenzaldehydes (**6a-b**) with 70–80% yield. The Baeyer Drewson Indigo Synthesis [15] was then employed to produce the 7,7′-dialkoxyindigoid (**2a-b**) with merely 12–18% yield.

The synthesis of 4,4′-dibromo-7,7′-dialkoxyindigoids (**3a-b**) were similar to the procedures described above with 3-alkoxybenzaldehyde (**5a-b**) employed as the starting material. Bromination was performed by adding liquid Br_2 to a chloroform solution of **5a-b** to give 2-bromo-5-alkoxybenzaldehyde (**7a-b**). The bromination gave out a single *ortho*-directing regioselective product **7a-b** with 87–92% yield [16]. Nitration was then carried out on **7a-b** to give 6-bromo-3-alkoxy-2-nitrobenzaldehyde (**8a-b**) with 72–80% yield. The Baeyer Drewson Indigo Synthesis was employed to synthesize 4,4′-dibromo-7,7′-dialkoxyindigoid (**3a-b**) with only 17–20% yield. The synthetic pathway is shown in Scheme 1.

The low yield for the Baeyer Drewson Synthesis in the last steps of the syntheses was suspected due to a mixed isomer were given out in the non-regioselective nitration reaction. Separation of the nitrated isomers before the final step, however, did not improve the yield significantly. Alternative cause would be the poor solubility of the compounds bearing the alkoxy side chains in the polar propanone/NaOH environment thus leading to a low yield. Aldol condensation of propanone itself could also lead to a formation of side products rather than the desired indigoids as well.

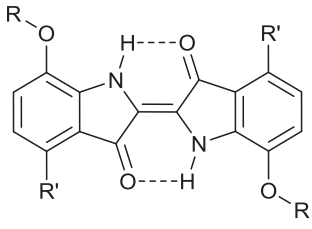

R = C_4H_9; R' = H , **2a**
R = C_8H_{17}; R' = H , **2b**
R = C_4H_9; R' = Br, **3a**
R = C_8H_{17}; R' = Br, **3b**

Fig. 2. Chemical structures of 7,7′-dialkoxyindigoids (**2a, 2b**) and 4,4′-dibromo-7,7′-dialkoxyindigoids (**3a, 3b**).

2.2. Electrochemical properties

Cyclic voltammetry (CV) measurement on compound **1** (indigo), **2a**, **2b**, **3a** and **3b** in DCM were effected using 0.1 M tetrabutylammonium hexafluorophosphate (Bu_4NPF_6) as the electrolyte. The sensitivity for the redox measurements were set initially at 1.0×10^{-5}A/V. Ferrocene was used as the internal standard and its HOMO was assigned to be −4.80 eV. The HOMO and LUMO energy levels were calculated according to the following equations:

$$\text{HOMO (eV)} = (E_{ox,\ onset} - E_{ox,\ onset,\ ferrocene}) + 4.8$$

$$\text{LUMO (eV)} = (E_{red,\ onset} - E_{ox,\ onset,\ ferrocene}) + 4.8$$

Compound **1** (indigo), together with the other four soluble indigoids (**2a-b, 3a-b**) all showed a characteristic double reduction signals (see Fig. 3). All these compounds consist of two analogous amide groups capable of forming mono- or di-amide anions when deprotonated (or reduced). The oxidative potentials, however, was insignificant to observe within the full scanning range from −1.8 V to 1.8 V using a sensitivity at 1.0×10^{-5}A/V partically for the highly insoluble indigo. The oxidative potentials of indigo, however, was only made observable when the sensitivity was increased to 1.0×10^{-6}A/V. The low oxidative intensity was due to the electron deficient nature of indigo and its derivatives. As these compounds are highly electron deficient, the removal of an extra electron (oxidation) from the molecules would be comparatively more difficult than the addition of electrons (reduction) into the molecules. As a result, the electron deficient nature make indigo and its derivatives an excellent n-type organic semicondutor.

The onset value of E_{ox} and E_{red} were estimated by extrapolating the linear regions from the curves in the cyclic voltammograms. The CV measured HOMO/LUMO (eV) for **1** (indigo), **2a-b**, **3a-b** and their corresponding bandgap (E_g, in eV) are listed in Table 1.

As seen in Table 1, the 7,7′-dialkoxyindigoids (**2a, 2b**) and 4,4′-Dibromo-7,7′-dialkoxyindigoids (**3a, 3b**) all shown a decreased LUMO compared to its parent reference compound **1** (indigo). The HOMO on the other hand, remained more of less unchanged for the two series of indigoids. The reduced LUMO level led to decreased bandgap energies for compounds **2a-b** and **3a-b**. Hydrocarbon substituents such as alkoxy and alkyl chains have been reported to reduce the bandgap energy in semiconductive materials such as polythiophenes and polythiazoles [17]. The narrowing of bandgap energies in indigoids is in agreement with the aforementioned examples. In both cases, the introduction of alkoxy groups lowered the bandgap of **2a-b** by 0.17–0.20 eV, while the bandgap of **3a-b** were further lowered by 0.22–0.25 eV.

4,4′-Dibromo-7,7′-dialkoxyindigoids (**3a, 3b**) have the lowest bandgap energies reported. The additional electron-withdrawing bromine atoms on **3a-b** could have further lower the LUMO [18] by making the indigoid core even more electron deficient. This type of indigoid was considered to be the most electron deficient among the different indigo species discussed in this article.

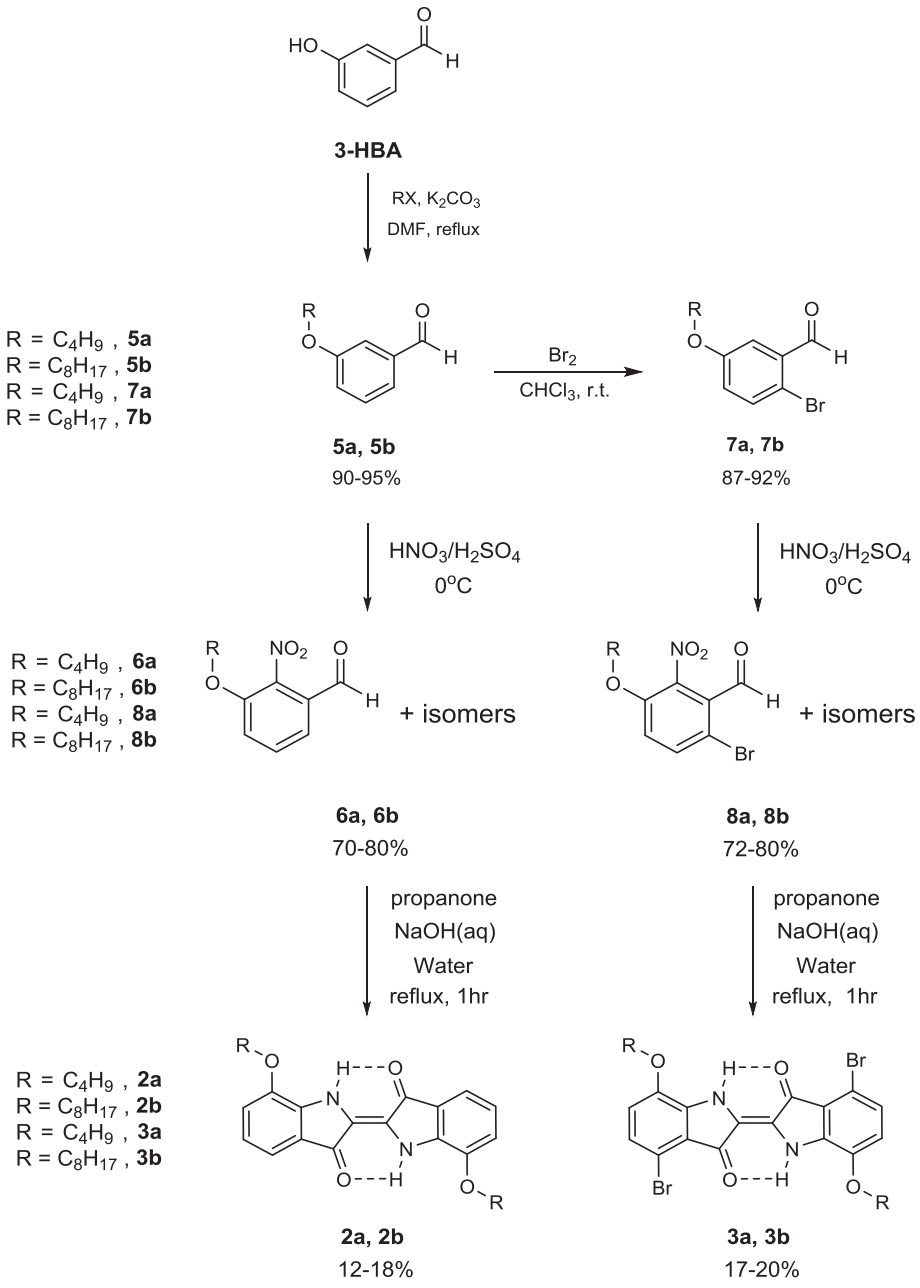

Scheme 1. Synthetic routes for the organic soluble indigoids.

2.3. Optical properties

The UV-vis absorptions for all compounds were measured in 10–50 ppm chloroform solutions at room temperature. The UV-vis spectra for the soluble indigoids (**2a**, **2b**, **3a** and **3b)** were shown in comparison to **1** (indigo) in Fig. 4. All of the samples showed intense absorptions in the orange-red domain of the visible light region. The absorptions were attributed to the $\pi \rightarrow \pi^*$ transition [19,20]. All soluble indigoids exhibited a broadened and red-shifted absorption with respect to **1** (indigo). A higher full-width-half-maxima (FWHM) value indicating the presence of auxochromic effect in the soluble indigoids exerted by either the alkoxy or bromo moieties on the compounds. The λ_{max} and other optical data of each sample were summarized in Table 2. Compound **4** will be further discussed in the following X-Ray crystallography section as it was used as a reference compound for the study of hydrogen bond effects on the stacking of indigoids.

It was observed that compound **2a**-**b** had a 28–30 nm red-shifted in the absorption maximum from indigo. A red-shift in absorption was mainly due to the auxochromic effect of the alkoxy groups present on the indigoid core. However, the peak broadening of indigoids comparative to indigo suggested that the material is either having an improved π-bonds conjugation [21] or probably π-π stacking [22]. The observation is similar to the side-chain effects in solid state polyhexylthiophenes [23]in which π-π stacking enhancement was a result of phase segregation between the hydrocarbon moieties and the aromatic thiophenes. The introduction of alkoxy groups onto the indigo aromatic rings also lowered the optical bandgap. Taking compound **2a-b** as an example, their bandgap energy reduced by approximately 0.13–0.14 eV in

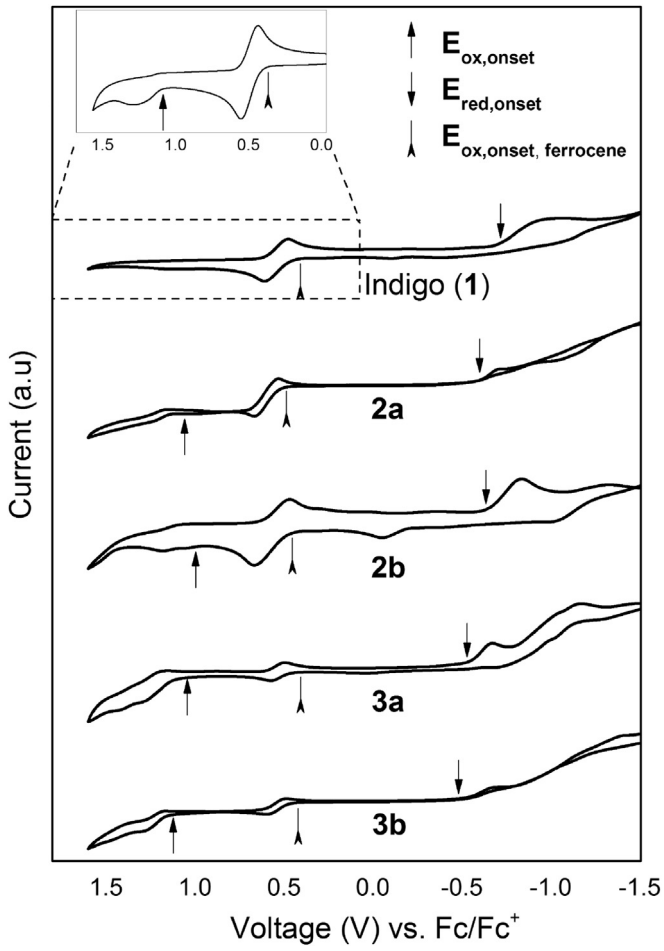

Fig. 3. Cyclic voltammograms of **1** (Indigo), **2a**, **2b**, **3a** and **3b** with ferrocene as an internal standard. The arrows indicating the oxidation and reduction transition regions.

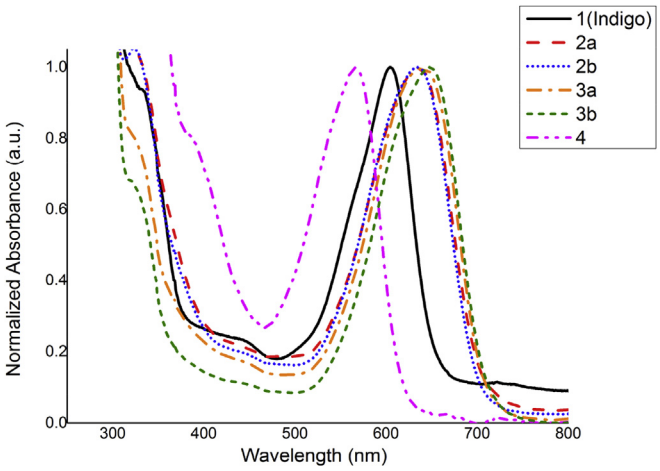

Fig. 4. Normalized UV-vis absorption spectra of **1** (indigo), **2a**, **2b**, **3a** and **3b**. Compound **4** would be introduced in the next sections.

Table 2
UV-vis data of indigo and indigoids.[a]

Compound	λ_{max} (nm)	λ_{edge} (nm)	FWHM[c] (nm)	E_g[b] (eV)
1	605	651	72	1.90
2a	635	702	99	1.77
2b	633	706	99	1.76
3a	640	707	95	1.75
3b	649	707	96	1.75

[a] Measurements were performed in chloroform solutions using a 1 cm quartz cuvette at room temperature.
[b] E_g was the optical bandgaps calculated from the absorption edges.
[c] FWHM were estimated by the curve fitting function in the software OriginPro 9.0 by assuming the spectra followed the Gaussian system.

comparison to **1** (indigo) (see Table 2). The results were consistent with the electrochemical bandgap energy estimated from cyclic voltammetry.

Compounds **3a-b** have the largest red-shift in their absorption maximum. Their absorption maxima were red-shifted by 35–44 nm from indigo (**1**). A higher red-shift was conceivably due to the synergistic effect of electron deficiency alkoxy and bromo substituents. The extension of π system caused by the overlapping *p*-orbital on the bromine substituents may also play a role in the observed red-shift. The bandgap energy of **3a-b** was further lowered by approximately 0.15 eV from **1** (indigo) (see Table 2). The results were also in agreement with the CV data for compounds **3a-b** which have the lowest bandgap energy among the samples studied.

2.4. Solubility

Solubility of the indigoids was validated by visual inspection on the color of a solution containing 5 mg of the samples in 1 mL of the solvent. The solution was first transferred to the top of a ~1 cm silica gel column and was flushed down under an applied pressure. The indigoids that are considered as soluble would pass through the silica gel with their color retained, while insoluble indigoids would have the color reside on top of the silica gel and only a colorless filtrate was collected. Slightly soluble samples would produce a pale blue filtrate even after successive washing with the solvent. The solubility of the indigoids using different solvents is summarized in Table 3.

Table 1
Electrochemical data of indigo and the indigoids.[a]

Compound	$E_{ox,\ onset}$ (V)	$E_{red,\ onset}$ (V)	$E_{ox,\ onset,\ ferrocene}$ (V)	HOMO (eV)	LUMO (eV)	E_g[b] (eV)
1[c]	1.106	−0.803	0.449	−5.46	−3.55	1.91
2a	1.140	−0.599	0.518	−5.42	−3.68	1.74
2b	1.027	−0.678	0.480	−5.35	−3.64	1.71
3a	1.116	−0.540	0.462	−5.45	−3.80	1.66
3b	1.162	−0.527	0.464	−5.50	−3.81	1.69

[a] Measurements were performed in degassed DCM solutions with 0.1 M tetrabutylammonium hexafluorophosphate as the electrolyte and ferrocene as the internal standard at room temperature.
[b] E_g was the electrochemical bandgaps calculated from the difference of the HOMO LUMO.
[c] As compound **1** (indigo) was only slightly soluble in DCM, the solution for **1** was slightly warmed and sonicated before the CV measurements in DCM.

It had been reported that the poor solubility of indigo was caused by strong intermolecular hydrogen-bonds. The enhanced solubility of the indigoids (**2a-b**, **3a-b**) was suggested to be a result of the removal of the intermolecular hydrogen-bonds. An effective intramolecular hydrogen-bond, however, should be preserved in order for the stacking of the indigoids molecules to show the OFET field-effect. The preservation and removal of inter- and intramolecular hydrogen-bonds were confirmed using single crystal x-ray crystallography to be discussed in the following section.

2.5. X-ray crystallography analysis

In order to examine the effects of inter- and intramolecular hydrogen-bonds on solubility and field-effect of the indigoids, single crystal X-Ray analyses were performed on a selected indigoid (**2a**) and a reference compound (**4**). The reference compound *N-N′*-dihexanoylindigoid (**4**) was synthesized by acylation of compound **1** (indigo) with hexanoyl chloride (see Scheme 2). The hexanoyl moiety allows indigoid (**4**) to be soluble yet at the same time eliminated the possibility of inter- and intramolecular hydrogen-bonds.

Single crystals of compound **2a** and **4** were grown in chloroform using hexane as the anti-solvent. The crystal growth took place within 1–2 days under dark. The crystal structure of **2a** and **4** were shown in Fig. 5. Their images were resolved by an X-ray analysis software Olex2 [24].

As shown in Fig. 5, the presence of intramolecular hydrogen-bonds in **2a** showed a completely different geometry from **4**, as the later compound had all of its hydrogen-bonds removed by acylating of the analogous amides on its indigo core. For compound **2a**, the atom-to-atom distance between the analogous amide hydrogen and carbonyl oxygen was estimated to be 2.386 Å. The distance was categorized as a "strong, mostly covalent" donor-acceptor distance according to George A. Jeffrey [25]. The strong intramolecular hydrogen-bonds in **2a** provided a rigid and planar molecular geometry between the two indoxyl rings as shown by the single crystal X-Ray crystallography. The bulky butoxy groups on the 7 and 7′ position of **2a** provided a steric effect to eliminate intermolecular hydrogen-bonds between individual indigoid molecules, and thus afforded the soluble indigoid **2a**. Moreover, a new pair of "moderate" [25] intramolecular hydrogen-bonds with atom-to-atom distance of 2.674 Å was also observed between the butoxy oxygen atom and the analogous amide hydrogen atom on compound **2a**.

In compound **4**, the two amide hydrogen atoms on indigo were substituted by two hexanoyl group, rendering it soluble in most organic solvents. The central double bond on **4**, however, was greatly twisted. The two hydrophobic hexanoyl chains also tended to align to one another, making the two indoxyl rings bent into a "butterfly" geometry. As a result, the planarity of the indigo core was completely destroyed.

At the same time, OFET devices were fabricated to correlate the influence of hydrogen-bonds on their field-effect properties. A summary on the hydrogen-bonds on solubility and exhibition of field-effects were given in Table 4. Interestingly, it was found that intramolecular hydrogen-bonds within indigo or indigoids were crucial for the exhibition of field-effect in OFET. As discussed earlier, the intramolecular hydrogen-bonds preserved planarity of the indigo core and is one of the major factors for a working indigoid-based OFET. Intermolecular hydrogen-bonds, however, only made the indigoid insoluble. The natural occurring compound **1** (indigo) would be of such case.

As seen in Fig. 4 previously, the UV-vis absorption for **4** was found to have a significant blue-shift from **1** (indigo). The blue-shift was probably attributed to the loss of the intra-molecular hydrogen-bonds as the two indoxyl rings within **4** became no longer co-planar, and therefore shortened the π-conjugation within the compound. This is in consistent with its x-ray structure. The

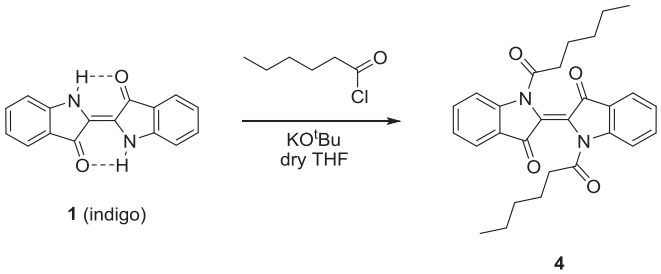

Scheme 2. Synthesis of *N-N′*-dihexanoylindigoid (**4**).

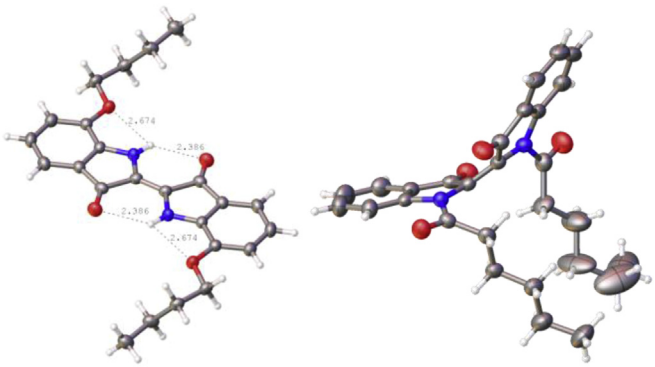

Fig. 5. Molecular structure of **2a** and **4**.

Table 4
Effect of hydrogen bonds on solubility and OFET field-effect of indigo and their derivatives.

Compound	Inter. H-bonds	Intra. H-bonds	Solubility	Field-effect
1	+	+	−	+
2a	−	+	+	+
4	−	−	+	−

Notes: + and − indicate the presence and absence of H-bonds, field-effect in OFET and soluble or insoluble in common organic solvents.

Table 3
Solubility of indigo and indigoids in various solvents.

Compound	$CHCl_3$	DCM	THF	EA	DMF	Acetone	Hexane	MeOH	H_2O
1	INS[a]	INS[a]	INS[a]	INS[a]	SS	INS	INS	INS	INS
2a	S	S	S	S	S	SS	INS	INS	INS
2b	S	S	S	S	S	SS	INS	INS	INS
3a	S	S	S	S	S	S	SS	INS	INS
3b	S	S	S	S	S	S	SS	INS	INS

Notes: "S" indicates completely soluble; "SS" indicates slightly soluble; "INS" indicates insoluble.
[a] Solution becomes slightly soluble upon slightly warmed and sonicated.

CCDC numbers and other crystal packing images of compound **2a** and **4** can be found in the electronic supplementary materials of this paper.

2.6. OFET measurements

The suitability of the soluble indigoids applied as n-type organic semiconductor was demonstrated using a bottom-gate-top-contact (BGTC) configuration OFETs (see Fig. 6). Polystyrene (PS) (MW ~35,000) was selected as the dielectric layer. A 30 mg/mL PS solution in chlorobenzene was spin-coated on a pre-cleansed *p*-doped SiO_2 substrate under nitrogen atmosphere and then vacuum dried. The active layer, either compound **1** (indigo), **2a**, **3a**, **3b** or **4,** was vacuum deposited on top of the dried polystyrene layer using an Edwards (Auto 306A) evaporator. The same fabrication conditions were employed in order to compare the results with the benchmark compound **1** (indigo). Al/LiF was used as the source/drain electrodes and the channel width for all OFET devices was 50 μm.

Both indigoid series exhibited characteristic n-channel field-effect behaviour (see Fig. 7). Under an applied gate voltage (V_G), the charge carriers, in this case electron, were accumulated at the indigoid/PS interface. An effective resistance was created as electrons travelled through the semiconducting active layer. As a result, the current (I_{DS}) flowing from source to drain was regulated by the source/drain voltage (V_{DS}) and the overall electron flows can be modulated by the gate voltage (V_G). The carrier mobility was calculated at the saturated regime from the output curves (horizontal regions from the V_{DS} vs I_{DS} curves in Fig. 7). The electron mobility and current on/off ratio measured for the different indigoids are summarized in Table 5. As expected, compound **4** did not exhibit any field-effect behaviour and its results were not presented.

The electron mobilities for the soluble indigoids are within the same order of magnitude compared to **1** (indigo). The mobility measured for all compounds (including indigo), however, are much lower than the literature reported value ($\mu_{Sat} = 0.02$ cm^2V^{-1} s^{-1} for indigo [3]). It has been suggested that the performance for OFET can be greatly affected by the selection of the dielectric layer [26]. A range of dielectric materials including vinyl polymers, crosslinkable polymer precursor benzocyclobutene (BCB), and paraffin waxes were studied for their effects on the performance of indigo-based OFETs. As a result, electron mobility ranged from $<10^{-4}$ to 10^{-3} cm^2 V^{-1} s^{-1} were detected. Recently, dielectric layer based on a long aliphatic hydrocarbon chain, such as tetratetracontane (TTC), was used as a template to induce the formation of a crystalline structure for the indigo layer. An improvement in charge transport properties resulted in OFETs [26] with highest μ_{sat} at 9.1 cm^2 V^{-1} s^{-1} was reported. Therefore, the selection of a suitable and compatible dielectric layer is crucial for a high performance indigoid-based OFET. It is suggested either a photo-cured dielectric layer or an inverted gate configuration would be used in future for the optimization of the solution processed indigoid-based OFET devices. The transistor transfer characteristic curves of OFET devices based on **1** (indigo), **2a, 3a** and **3b** can be found in the supplementary materials of this article.

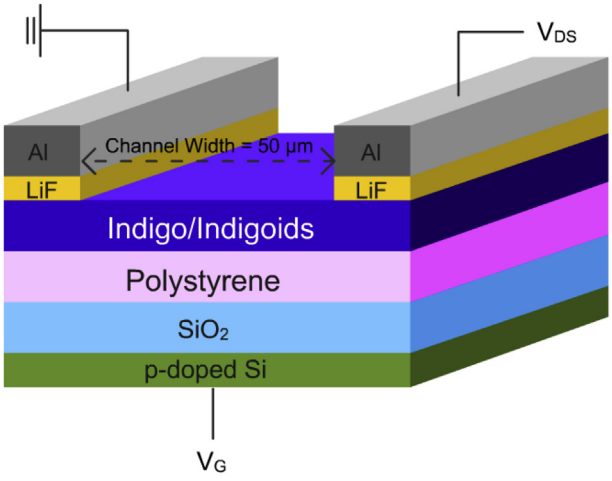

Fig. 6. Configuration of a bottom-gate-top-contact (BGTC) OFET device.

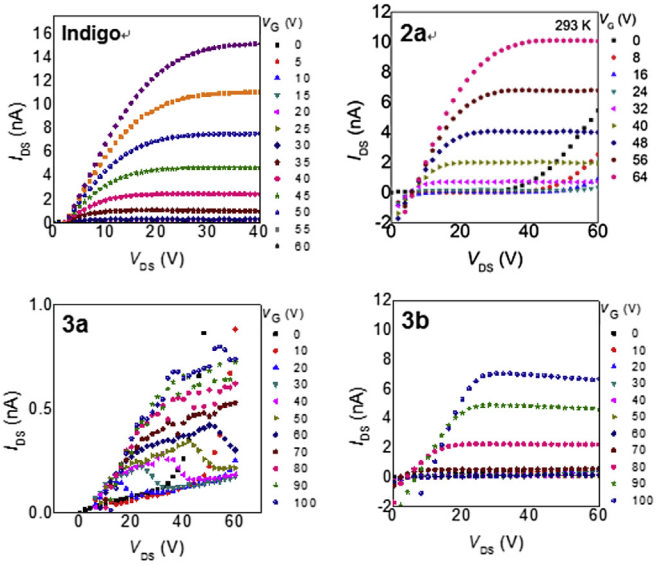

Fig. 7. Output curves of OFET devices based on **1** (indigo), **2a, 3a** and **3b** measured at ambient temperature. Compound **3a** showed a weaker transistor field-effect.

Table 5
Electron mobility of indigo and indigoids.

Compound	S/D electrode	μ_{Sat} (cm^2V^{-1} s^{-1})	$I_{on/off}$
1 (Indigo)	Al/LiF	2.40×10^{-5}	6.1×10^2
2a	Al/LiF	1.66×10^{-5}	1.8×10
3a	Al/LiF	4.80×10^{-6}	N/A
3b	Al/LiF	2.20×10^{-5}	1.6×10^2
4	Al/LiF	No field-effect observed	No field-effect observed

3. Experimantal

3.1. Characterization

^1H and ^{13}C NMR spectra were recorded with a Bruker-AF301 AT 400 MHz spectrometer using $CDCl_3$ or acetone-d_6 as solvent and tetramethylsilane as the internal standard. High resolution mass spectrometry (HRMS) was carried out using a Bruker autoflex MALDI-TOF mass spectrometer. Cyclic voltammetry (CV) measurements were performed on a BAS CV-50W electrochemical analyzer adapted with a conventional three-electrode configuration consisting platinum working and auxiliary electrodes and a Ag/AgCl reference electrode. The measurements were carried out in 0.1 M DCM solution with tetrabutylammonium hexafluorophosphate as the electrolyte and ferrocene as the internal standard. UV-vis absorption spectra were measured in chloroform a Cary UV-100 (Double Beam) spectrophotometer. Single-crystal structural determination was performed using a Single-Crystal X-

Ray Diffractometer (Smart 1000 with CCD Area Detector).

3.2. Materials

Indigo, 3-hydroxybenzaldehyde, 1-bromobutane, 1-bromooctane, bromine, potassium carbonate, sodium hydroxide were purchased from Sigma Aldrich. Other solvents were analytical grade and used as received.

3.3. Synthesis of indigoids

3-alkoxybenzaldehyde (5a-b): To a 500 mL round bottom flask, 10 g (0.0819 mol) of 3-hydroxybenzaldehyde (**3-HBA**) was dissolved in 150 mL dimethylformamide. 22.6 g (0.164 mol) potassium carbonate was added to the solution of **3-HBA**. 9.73 mL (0.0901 mol) of 1-bromobutane was added in one portion to the reaction mixture. The mixture was fitted with a condenser and was heated to 160 °C with a sand bath. The reaction was stirred vigorously with a magnetic stirring bar with heating for 30 min. The reaction temperature was then lowered to room temperature. 200 mL water was added to the mixture followed by 100 mL of hexane. The solution was then stirred at room temperature until the excess potassium carbonate powder was dissolved in the aqueous layer. The solution was then transferred to a separating funnel, and 100 mL of hexane was added. The aqueous layer was discarded and the organic layer was washed with 10% HCl solution, water and finally with saturated NaCl solution. The organic layer was collected and anhydrous Na_2SO_4 or anhydrous $MgSO_4$ was added to remove residue of water in the organic solution. The desiccation salt was removed by filtration and the filtrate was collected. Chloroform was used to rinse any remaining product adhered on the salt and flask. The solvent was then removed by rotary evaporation, and dried in vacuo to obtain a pale yellow oily liquid of 3-butoxybenzaldehyde (**5a**) (13.9 g, 95%). δ_H (Acetone-d_6) 0.97 (3H, t, *J* 7.4, CH_3), 1.46–1.56 (2H, m, butoxy CH_2), 1.74–1.81 (2H, m, butoxy CH_2), 4.07 (2H, t, *J* 6.4, OCH_2), 7.23–7.26 (1H, m, ArH), 7.43 (1H, d, *J* 2.6, ArH), 7.49–7.51 (2H, m, ArH) and 10.0 (1H, s, CHO); δ_C (Acetone-d_6) 13.26, 19.01, 31.09, 67.69, 113.27, 121.18, 122.31, 130.16, 138.22, 159.80, 191.89.

The synthesis of 3-(octyloxy)benzaldehyde (**5b**) was done by the same procedure described to synthesize 3-butoxybenzaldehyde (**5a**) except the alkyl halide used was 13.7 mL (0.0901 mol) of 1-bromooctane instead of 1-bromobutane. The product obtained was a pale yellow oily liquid of **5b** (17.3 g, 90%). δ_H ($CDCl_3$) 0.89 (3H, t, *J* 7.0, CH_3), 1.29–1.48 (10H, m, octyloxy CH_2), 1.76–1.83 (2H, m, octyloxy CH_2), 4.00 (2H, t, *J* 6.6, OCH_2), 7.15–7.18 (1H, m, ArH), 7.38 (1H, d, *J* 2.1, ArH), 7.42–7.43 (2H, m, ArH) and 9.96 (1H, s, CHO); δ_C ($CDCl_3$) 14.10, 22.66, 26.01, 29.13, 29.24, 29.33, 31.81, 68.26, 112.72, 121.91, 123.25, 129.96, 137.76, 159.71, 192.16.

2-bromo-5-alkoxybenzaldehyde (7a-b): To a 500 mL round bottom flask, 4 g (0.0224 mol) of 3-butoxybenzaldehyde (**5a**) was dissolved in 200 mL chloroform. 1377 μL (0.0269 mol) of liquid bromine was dissolved in 10 mL chloroform in a dropping funnel connected to the round bottom flask. The whole system was protected in nitrogen atomosphere. The bromine solution was slowly added to the alkoxybenzaldehyde solution via a dropping funnel over 30 min. The solution was kept at room temperature with stirring. After the complete addition of bromine, the reaction was stirred continuously for another 30 min 200 mL of cold water was added to stop the reaction. The mixture was transferred to a separating funnel. The crude product was extracted with chloroform and the aqueous layer was discarded. The organic layer was further washed with a 20% sodium thiosulfate solution to remove the remaining bromine. The product solution was then washed with concentrated NaCl solution and dried with anhydrous $MgSO_4$ to remove any water residue. The desiccation salt was removed by filtration and the filtrate was collected. Chloroform was used to rinse any remaining product adhered on the salt and flasks. The solvent was then removed by rotary evaporation, and dried in vacuo to obtain a yellow brown viscous liquid of 2-bromo-5-butoxybenzaldehyde (**7a**) (5.01 g, 87%). The product was used directly in the next step and NMR analysis without further purification by column chromatography. δ_H (Acetone-d_6) 0.97 (3H, t, *J* 7.4, CH_3), 1.46–1.55 (2H, m, butoxy CH_2), 1.74–1.81 (2H, m, butoxy CH_2), 4.07 (2H, t, *J* 6.4, OCH_2), 7.18 (1H, dd, *J* 8.8 and *J* 3.2, ArH), 7.36 (1H, d, *J* 3.2, ArH), 7.63 (1H, d, *J* 8.8, ArH) and 10.25 (1H, s, CHO); δ_C (Acetone-d_6) 13.19, 18.91, 30.94, 68.10, 113.84, 116.44, 122.85, 134.14, 134.75, 159.02, 190.81.

The synthesis of 2-bromo-5-(octyloxy)benzaldehyde (**7b**) was done by the same procedure described to synthesize 2-bromo-5-butoxybenzaldehyde (**7a**) except the 3-alkoxybenzaldehyde used was 5.25 g of 3-(octyloxy)benzaldehyde (**5b**) instead of **5a**. The product given out was a yellow liquid of 2-bromo-5-(octyloxy) benzaldehyde (**7b**) (6.46 g, 92%). δ_H (Acetone-d_6) 0.88 (3H, t, *J* 6.8, CH_3), 1.26–1.52 (10H, m, octyloxy CH_2), 1.76–1.83 (2H, m, octyloxy CH_2), 4.07 (2H, t, *J* 6.5, OCH_2), 7.19 (1H, dd, *J* 8.8 and *J* 3.2, ArH), 7.37 (1H, d, *J* 3.2, ArH), 7.64 (1H, d, *J* 8.8, ArH) and 10.26 (1H, s, CHO); δ_C (Acetone-d_6) 14.37, 23.32, 26.67, 29.79, 30.00, 32.57, 69.32, 114.81, 117.32, 123.76, 135.08, 135.67, 159.96, 191.71.

3-alkoxynitrobenzaldehyde (6a-b) and 2-bromo-5-alkoxynitrobenzaldehyde (8a-b): To a 100 mL conical flask, 1523 μL (0.0218 mol) 65% nitric acid was slowly added to 20 mL (0.364 mol) 96% concentrated sulfuric acid at 0 °C to make up the nitrating reagent. The solution was stirred in an ice bath for 10 min. It was added 3 g (0.0168 mol) of 3-butoxybenzaldehyde (**5a**) dropwise to the nitrating reagent in 30 min via a dropping funnel. The solution was kept stirring at 0 °C for 30 min. Crushed ice was added directly to the reaction mixture to precipitate the nitration product. The crude product was collected by suction filtration and washed with cold water. The crude product was dried in a vacuum oven at room temperature to obtain a yellow powder of 3-butoxynitrobenzaldehyde (**6a**) (3 g, 80%) and was used directly in the next step without further purification.

The syntheses of 3-(octyloxy)nitrobenzaldehyde (**6b**), 6-bromo-3-butoxynitrobenzaldehyde (**8a**) and 6-bromo-3-(octyloxy)nitrobenzaldehyde (**8b**) were done by the same procedure described to synthesize 3-butoxynitrobenzaldehyde (**6a**) except the benzaldehyde used was 3.94 g (0.0168 mol) of 3-(octyloxy)benzaldehyde (**5b**), 5.5 g (0.0168 mol) of 2-bromo-5-butoxybenzaldehyde (**7a**) or 5.26 g (0.0168 mol) of 2-bromo-5-(octyloxy)benzaldehyde (**7b**) instead of **5a**. The products **6b** (3.28 g 70%), **8a** (4.06 g, 80%) and **8b** (4.33 g, 72%) obtained were all yellow powder and were used directly in the next step without further purification or NMR analyses.

7,7′-dialkoxyindigoids (2a-b) and 4,4′-dibromo-7,7′-dialkoxyindigoids (3a-b): To a 100 mL round bottom flask, 2 g of the crude product of 3-butoxynitrobenzaldehyde (**6a**) was dissolved in 30 mL propanone. The mixture was cooled to -5 °C with an ice/$CaCl_2$ bath for 15 min. A solution of 4 mL 0.2 N sodium hydroxide solution was added slowly to the propanone mixture with a dropping funnel under moderate stirring. Upon the solution turned deep red in color, 30 mL 0.4 N sodium hydroxide solution was added slowly using a dropping funnel. The reaction mixture was stirred for another 15 min. The temperature of the reaction mixture was then raised to room temperature. When the mixture turned deep green in color, the reaction mixture was further increased to refluxing temperature and stirred for an additional 1 h. The temperature was lowered to room temperature and 30 mL of methanol was added to quench the reaction. The reaction mixture was cooled to 0 °C with an ice bath and stirred for 15 min. The crude product was filtered

with suction filtration, washed with cold water and methanol, and allowed to dry in a vacuum oven to obtain blue solids of 7,7′-dibutoxyindigoid (**2a**). The blue solids were purified by flash column chromatography using toluene as eluent. The final purified product of **2a** (656 mg, 18%) were blue shiny crystalline needles. δ_H ($CDCl_3$) 1.02 (6H, t, *J* 7.4, CH_3), 1.51–1.60 (4H, m, butoxy CH_2), 1.82–1.89 (4H, m, butoxy CH_2), 4.10 (4H, t, *J* 6.4, OCH_2), 6.90 (2H, t, *J* 7.8, ArH), 6.99 (2H, dd, *J* 7.8 and *J* 0.7, ArH), 7.31 (2H, dd, *J* 7.6 and *J* 0.7, ArH) and 8.92 (2H, s, NH); δ_C ($CDCl_3$) 13.88, 19.32, 31.18, 68.51, 115.71, 116.82, 120.80, 121.10, 121.75, 142.69, 145.50, 188.90; MALDI-TOF-MS Calculated [M + H^+]: 407.1965; Found: 407.1963.

The syntheses of 7,7'dioctyloxyindigoid (**2b**) was done by the same procedure described to synthesize 7,7′-dibutoxyindigoid (**2a**) except the nitrobenzaldehyde used were 2 g **6b**. The product **2b** (446 mg, 12%) obtained were blue shiny crystalline needles. δ_H ($CDCl_3$) 0.90 (6H, t, *J* 6.8, CH_3), 1.25–1.60 (20H, m, octyloxy CH_2), 1.83–1.90 (4H, m, octyloxy CH_2), 4.08 (4H, t, *J* 6.6, OCH_2), 6.90 (2H, t, *J* 7.7, ArH), 6.97 (2H, d, *J* 7.7, ArH), 7.31 (2H, d, *J* 7.6, ArH) and 8.92 (2H, s, NH); δ_C ($CDCl_3$) 14.14, 22.69, 26.07, 29.15, 29.26, 29.38, 31.86, 68.80, 115.68, 116.79, 120.78, 121.08, 121.72, 142.64, 145.49, 188.89; MALDI-TOF-MS Calculated [M^+]: 518.3145; Found: 518.3133.

The synthesis of 4,4'dibromo-7,7′-dibutoxyindigoid (**3a**) and 4,4'dibromo-7,7′-dioctyloxyindigoid (**3b**) were done by the same procedure described to synthesize 7,7′-dialkoxyindigoids (**2a-b**) except the nitrobenzaldehyde used were 2 g of 2-bromo-5-butoxybenzaldehyde (**8a**) or 2 g of 2-bromo-5-octyloxynitrobenzaldehyde (**8b**). The final product obtained from **8a** was a bluish purple powder of **3a** (747 mg, 20%). δ_H ($CDCl_3$) 1.00 (6H, t, *J* 7.3, CH_3), 1.49–1.58 (4H, m, butoxy CH_2), 1.80–1.87 (4H, m, butoxy CH_2), 4.05 (4H, t, *J* 6.5, OCH_2), 6.78 (2H, d, *J* 8.4, ArH), 6.97 (2H, d, *J* 8.4, ArH) and 8.98 (1H, s, NH); δ_C ($CDCl_3$) 13.87, 19.30, 31.11, 68.80, 109.22, 117.42, 118.19, 121.59, 124.86, 134.95, 144.89, 186.60; MALDI-TOF-MS Calculated [M + H^+]: 565.0157; Found: 565.0166.

The Baeyer-Drewson product obtained from **8b** was a bluish purple powder of **3b** (642 mg, 17%). δ_H ($CDCl_3$) 0.90 (6H, t, *J* 6.6, CH_3), 1.31–1.51 (20H, m, octyloxy CH_2), 1.80–1.87 (4H, m, octyloxy CH_2), 4.03 (4H, t, *J* 6.6, OCH_2), 6.77 (2H, d, *J* 8.4, ArH), 6.96 (2H, d, *J* 8.3, ArH) and 8.97 (2H, s, NH); δ_C ($CDCl_3$) 14.15, 22.69, 26.02, 29.10, 29.23, 29.36, 31.86, 69.14, 109.17, 117.37, 118.15, 121.50, 124.82, 143.88, 144.86, 186.43; MALDI-TOF-MS Calculated [M + Na^+]: 699.1229; Found: 699.1268.

N-N′-dihexanoylindigoid (4): To a 250 mL round bottom flask, 3 g (0.0114 mol) of compound **1** (indigo) was dissolved in 100 mL dry THF and was degassed for 10 min using a sonicator. The solution was then protected in nitrogen atmosphere, followed by the addition of 4.38 g (0.0456 mol) of sodium tert-butoxide in a single portion. The reaction mixture was stirred vigorously at room temperature for 15 min. A solution of 4780 μL (0.0342 mol) of hexanoyl chloride was added slowly to the solution. The reaction mixture was heated at 60 °C for 30 min with an oil bath in nitrogen atmosphere. Once the solution turned deep purple in color, the reaction mixture was cooled to room temperature. 50 mL chloroform was added to the mixture and the purple slurry was filtered and washed with chloroform to remove any organic insoluble side products. The filtrate was collected and transferred to a separating funnel. The organic portion was washed with 20% sodium bicarbonate solution to remove any unreacted acid. The organic layer was washed 3 times with water to remove any water soluble impurities. The aqueous layer was discarded and the organic layer was collected. Anhydrous $MgSO_4$ was added to the product solution to remove residue of water. The desiccation salt was removed by simple filtration and the filtrate was collected. Chloroform was used to rinse any remaining product adhered on the $MgSO_4$ salt and flask. The solvent was then removed by rotary evaporation to obtain a reddish pink powder. N-N'-dihexanoylindigoid (**4**) was then further purified with silica gel column chromatography with eluent of hexane: ethyl acetate = 4:1. The final product of compound **4** (1.47 g, 28%) was a reddish purple powder. δ_H ($CDCl_3$) 0.85 (6H, t, *J* 6.8, CH_3), 1.23–1.30 (8H, m, hexanoyl CH_2), 1.76–1.82 (4H, m, hexanoyl CH_2), 2.84 (4H, br, hexanoyl CH_2), 7.26 (2H, t, *J* 7.5, ArH), 7.63–7.67 (2H, m, ArH), 7.76 (2H, d, *J* 7.6, ArH), 8.24 (2H, d, *J* 8.1, ArH); δ_C ($CDCl_3$) 13.85, 22.41, 25.30, 31.41, 36.19, 117.00, 121.84, 124.35, 124.96, 125.99, 138.86, 149.37, 173.71, 184.15; MALDI-TOF-MS Calculated [M + Na^+]: 481.2103; Found: 481.2090.

4. Conclusions

We have reported the synthesis of two series of novel organic soluble indigoids namely 7,7′-dialkoxyindigoids (**2a, 2b**) and 4,4′-dibromo-7,7′-dialkoxyindigoids (**3a, 3b**) both started from the low-cost 3-hydroxybenzaldehyde. The indigoids are soluble in common organic solvents including chloroform, DCM, THF, EA and DMF. The HOMO/LUMO and bandgap energy (E_g) of the alkoxy and bromine substituted indogoids were all found to be lower than their parent indigo compound. The lowest HOMO/LUMO at −5.50 eV/−3.81 eV and the lowest reported bandgap energy (E_g) at 1.69 eV was found for compound **3a**.

By analyzing single-crystal x-ray crystallography for the indigoids, it was found that the presence of intramolecular hydrogen-bonds is crucial for the exhibition of field-effect behaviour, while intermolecular hydrogen-bonds lead to insolubility. Long alkoxy chain substituents at the 7 and 7′ positions on the indigo core effectively eliminated the intermolecular hydrogen-bonds for the purpose of improve solubility, and at the same time preserving intramolecular hydrogen-bonds necessary for field-effect behaviour.

The employment of the soluble indigoids as an active layer for n-type OFET have electron mobility ranged from 1.66×10^{-5} cm^2V^{-1} s^{-1} to 2.20×10^{-5} cm^2V^{-1} s^{-1} and is within the same order of magnitude for the pristine indigo fabricated under the same conditions and configuration. The values, however, are lower than those reported in literature and is suggested relating to the selection of the dielectric layer. Further device improvement included the use of a hydrophobic dielectric layer or employing a different device configuration would be the subject for further study. The bromine substituted **3a** and **3b** can be further functionalized and their chemistry and properties will also be reported in a future communication.

Acknowledgements

The authors gratefully acknowledge the support by the University Faculty Research Grant (FRG 1/14-15/046). The authors also thank Dr. Zhu Nianyong from Prof. Wong Wai-yeung's research group for the X-ray crystallography measurements.

Appendix A. Supplementary data

Supplementary data related to this article can be found at http://dx.doi.org/10.1016/j.orgel.2016.02.035.

References

[1] Bernard T. Golding, Colin Pierpoint, Education in Chemistry, Adv. Mater (1986) 71–73.
[2] I.V. Klimovich, L.I. Leshanskaya, S.I. Troyanov, D.V. Anokhin, D.V. Novikov, A.A. Piryazev, D.A. Ivanov, N.N. Dremova, P.A. Troshin, J. Mater. Chem. C 2 (2014) 7621.
[3] Eric Daniel Gowacki, Gundula Voss, Lucia Leonat, Mihai Irimia Vladu, Siegfried Bauer, Niyazi Serdar Sariciftci, Isr. J. Chem. 52 (2012) 540.
[4] E.D. Glowacki, N.S. Sariciftci, G. Voss, K. Demirak, M. Havlicek, N. Sünger, A.C. Okur, U. Monkowius, J. Gasiorowski, L. Leonat, Chem. Commun. Camb.

Engl. 49 (2013) 6063.
[5] P.H.H. Gray, Proc. R. Soc. B Biol. Sci. 102 (1928) 263–280.
[6] R. Rondão, J.S. Seixas de Melo, V.D.B. Bonifácio, M.J. Melo, J. Phys. Chem. A 114 (2010) 1699.
[7] Yukihiro Matsumoto, Hitoshi Tanaka, Heterocycles 60 (2003) 1805–1810.
[8] Bradley D. Smith, David E. Alonso, Jeffrey T. Bien, John D. Zielinski, Sheridan L. Smith, Kenneth J. Haller, J. Org. Chem. 58 (1993) 6493–6496.
[9] Chang Guo, Bin Sun, Jesse Quinn, Zhuangqing Yan, Yuning Li, J. Mater. Chem. C 2 (2014) 4289–4296.
[10] Albrecht Schmidt, Process of Brominating Indigo, United States Patent Office, 1905.
[11] L.L. Lloyd, The Chemistry of Dyestuffs: A Manual for Students of Chemistry and Dyeing, 1917, pp. 270–272.
[12] M. Yao, K. Kuratani, T. Kojima, N. Takeichi, H. Senoh, T. Kiyobayashi, Sci. Rep. 4 (2014) 3650.
[13] Gondola Voss, Michael Gradzielski, Jiirgen Heinz, Helmut Reinked, Carlo Unverzag, Helvetica Chim. Acta 86 (2003) 1982–2004.
[14] L. Rubenstein, J. Chem. Soc. 127 (1925) 1998.
[15] A. von Baeyer, Ber Dtsch, Chem. Ges. 12 (1879) 1309.
[16] Willem A.L. van Otterlo, Joseph P. Michael, Manuel A. Fernandes, Charles B. de Koning, Tetrahedron Lett. 45 (2004) 5091–5094.
[17] Qingshuo Wei, Shoji Miyanishi, Erjun Zhou, Kazuhito Hashimoto, Keisuke Tajima, Synth. Met. 196 (2014) 139–144.
[18] Raghunath R. Dasari, Amir Dindar, Chi Kin Lo, Cheng-Yin Wang, Cassandre Quinton, Sanjeev Singh, Stephen Barlow, Canek Fuentes-Hernandez, John R. Reynolds, Bernard Kippelen, Seth R. Marder, Phys. Chem. Chem. Phys. 16 (2014) 19345–19350.
[19] J. Seixas de Melo, R. Rondao, H.D. Burrows, M.J. Melo, S. Navaratnam, R. Edge, G. Voss, J. Phys, Chem. 110 (2006) 13653–13661.
[20] S.R. Oakley, G. Nawn, K.M. Waldie, T.D. MacInnis, B.O. Patrick, R.G. Hicks, Chem. Commun. Camb. Engl. 46 (2010) 6753.
[21] D. Fichou, Handbook of Oligo- and Polythiophenes, Wiley-VCH, Weinheim, 1999.
[22] N.K. Al-Rasbi, C. Sabatini, F. Barigelletti, M.D. Ward, Dalton Trans. Camb. Engl. 2003) (2006) 4769.
[23] Wen Y. Huang, C.C. Lee, S.G. Wang, Y.K. Han, M.Y. Chang, J. Electrochem. Soc. 157 (9) (2010) B1336–B1342.
[24] O.V. Dolomanov, L.J. Bourhis, R.J. Gildea, J.A.K. Howard, H. Puschmann, J. Appl. Cryst. 42 (2009) 339–341.
[25] George A. Jeffrey, An Introduction to Hydrogen Bonding, Oxford University Press, 1997.
[26] D.V. Anokhin, L.I. Leshanskaya, A.A. Piryazev, D.K. Susarova, N.N. Dremova, E.V. Shcheglov, D.A. Ivanov, V.F. Razumov, P.A. Troshin, Chem. Commun. Camb. Engl. 50 (2014) 7639.